Proceedings of 2016 IEEE
International Conference on Mechatronics and Automation
August 7 - 10, Harbin, China

Real-time Collision Detection for Manipulators Based on Fuzzy Synthetic Evaluation

Xia Jing
School of Mechanical Engineering
Xi'an University of Science and Technology
Xi'an, Shaanxi Province, 710054, China
382327499@qq.com

Wu Guangxin, Li Chongyang, Liu Hong
State Key Laboratory of Robotics and System
Harbin Institute of Technology
Harbin, Heilongjiang Province, 150001, China
Wuguangxin1986@gmail.com

***Abstract* - To overcome the shortcoming that the collision detection method based on three-dimension model only depends on the shortest distance between components to determine collision, a novel collision detection method for manipulators is proposed to indicate how dangerous the current movement of the robot are to the surrounding objects. The method more comprehensively considers the effect of the shortest distance, motion state, braking performance of joints, robot control mode and the contact state on robot collision risk, obtains a robot collision risk index by using the fuzzy synthetic evaluation. At the same time, building the collision detection model by using sphere sweeping convex hulls (SSCH) improves the real-time of the collision detection. Finally, the proposed method is validated through simulations and experiments.**

Index Terms - Collision detection; fuzzy synthetic evaluation; sphere sweeping convex hulls; manipulators.

I. INTRODUCTION

Safety control strategy for robots coexisted with humans or fine equipment has been gathering increasing attention from both industrial and research communities. Collision detection (CD) is a crucial task for humanoid and industrial robots. The shortest distance between robots and the surrounding objects is calculated by using their 3D geometric models to determine collisions. The collision detection method based on 3D geometry model does not require additional hardware and can effectively detect collisions, however, the bottleneck of the method is a large amount of computation cost. The hierarchical bounding volume technology is generally used to overcome this shortcoming. The technology often employ a hierarchy of geometrical primitives to represent or bound objects. Several collision detection approaches using different bounding volumes have been proposed in different contexts. Typical bounding volumes include axis-aligned bounding boxes (AABB) [1]-[2], object-oriented bounding boxes (OOBB) [3], bounding spheres [4]-[5], swept-sphere volumes [6]-[9] and convex hulls [10]-[12]. Okada [1] develops a precise collision detection system for the humanoid robot HRP-2 using the AABB based collision detection method, and demonstrate that the AABB based collision detection method is much faster than other conventional bounding volume representations based methods. However the system reduces the motion ranges of compound joints, In 2006, Okada [2] presents a hybrid approach that uses both table based collision checking for the compound joints and online geometrical model checking with simplified link shapes for other joints to deal with the problem. Steinbach [4] proposes an algorithm for computing compact sphere tree hierarchies of the humanoid robot for the purpose of efficient collision detection and minimum distance computation. The bounding spheres are simple, but their accuracy is low. Kuffner et al. [12] propose an efficient collision detection algorithm using a fast distance determination method for convex hulls. The minimum distance determination methods for convex hulls can be classified into two types, one is based on the nearest feature, such as the Lin-Canny and V-Clip algorithm [13]; the other is based on the simplex descent algorithm, such as Gilbert-Johnson-Keerthi (GJK) and SOLID algorithm [14]-[16]. By comparison, convex hulls can build the more accurate collision model, but requires a large amount of data. Taubig et al.[15,16] present a real time collision detection method based on computing SSCH of all bodies and using the Gilbert-Johnson-Keerthi algorithm (GJK) as collision detect block for computing the distance between two objects. SSCH is the Minkowski-sum of a convex polyhedron and a ball. This representation can construct precise collision model with fewer points and has the properties of convex hulls. It is more efficiency than other representation.

The existing collision detection methods evaluate the collision risk of robots by calculating the nearest distances between the components. Obviously the collision risk degree not only depends on the nearest distance, but also depends on the braking performance of joints, contact state, motion state and control mode. Thus these methods can't objectively and accurately make a danger assessment. One main contribution of this paper is a collision detection method for manipulators based on fuzzy synthetic evaluation. The method comprehensively considers five factors, such as, nearest distance, braking performance, contact state, movement state and control mode of manipulators. By using the fuzzy synthetic evaluation method, a new mathematical model is established to judge the collision risk degree of the manipulator, in order to determine whether braking must be triggered or not.

The paper is organized as follows. After we deliver insight into the applied distance computation algorithm which provides information about potentially colliding links in real-

978-1-5090-2396-7/16/$31.00 ©2016 IEEE

Authorized licensed use limited to: University of Florida. Downloaded on January 14,2021 at 17:31:59 UTC from IEEE Xplore. Restrictions apply.

time in Section II. Section III presents a collision detection method based on the fuzzy synthetic evaluation to compute the collision risk degree of manipulators. Section V presents the simulation and experimental results to demonstrate the validity of the novel method.

II. Security Distance Computation

A. *Braking Distance of Joints*

At high speeds, the braking distance of joints is one of the important factors affecting robot security. The existing research has usually added safety margins around each link to cope with the influence of the braking distance. However, such margins significantly decrease the movement range of joints. The braking distance is depended on joint angle velocity, acceleration, latency and the worst case deceleration, as well as joint angle uncertainties. We introduce the braking model of a single revolute joint by assuming a) The joint stays at the current movement state during a latency consisting of a cycle time and a communication time and b) the process of braking is a uniformly decelerated motion, and the braking of the joint thereafter is at worst a deceleration of $a_B = 1200^\circ / s^2$. Then, according to (1), the braking distance of each joint is exactly computed to safeguard whole braking movement.

$$\begin{aligned} \theta_i^1 &= \theta_i + \frac{\dot{\theta}_i + \dot{\theta}_i^1}{2} t_L + \frac{\dot{\theta}_i^1 \left| \dot{\theta}_i^1 \right|}{2a_B} \\ \dot{\theta}_i^1 &= \dot{\theta}_i + \ddot{\theta}_i t_L \end{aligned} \tag{1}$$

where θ_i, $\dot{\theta}_i$ and $\ddot{\theta}_i$ are the current joint angle, velocity and acceleration of the i-th revolute joint, θ_i^1 is the joint angle when the joint stops braking.

B. *Security Nearest Distance Computation*

The novel method first computes the swept volumes of whole braking movement, then the security distances between all pairs of swept volumes are computed by using the GJK-algorithm. The swept volumes of manipulators are represented by SSCH. For example, a manipulator consists of two links, the braking trajectory of the joint 1 is a circular arc (see Fig.1), which can be contained in a SSCH. The SSCH is defined as

$$\begin{aligned} &Circ(\alpha_0, \alpha_1, (r; [p_l]_{l=1}^n)) = V(r + f\max|p_l|; \\ &\left[p_l^0 + fp_l^{1/2}, p_l^1 + fp_l^{1/2} \right]_{l=1}^n) \end{aligned} \tag{2}$$

With

$$\varphi = \frac{\alpha_1 - \alpha_0}{2}, f = \frac{1-\cos\varphi}{2}, p_l^{1/2} = T(\alpha_0 + \varphi) p_l$$

where $T(\alpha_0 + \varphi)$ is transition matrix of the revolute joint. However the actual braking trajectory of the joint 2 is not known, we will approximate the actual braking trajectory by assuming that the manipulator links move separately according to priority order. The swept volumes of the braking movement can be obtained

$$\begin{aligned} &Circ \subset Circ1(\alpha_0, \alpha_1, (r; [p_l]_{l=1}^n)) + \\ &Circ2(\alpha_2, \alpha_3, (r; [p_l]_{l=1}^n) \end{aligned} \tag{3}$$

The tight bound of circular arc Circ1 and Circ2 is obtained by using (4), formally:

$$\begin{aligned} Circ1(\alpha_0, \alpha_1, (r; [p_l]_{l=1}^n)) &= V1(r_1; [p_l^0, p_l^1]_{l=1}^n) \\ Circ2(\alpha_2, \alpha_3, (r; [p_l]_{l=1}^n)) &= V2(r_2; [p_l^2, p_l^3]_{l=1}^n) \end{aligned} \tag{4}$$

Thus

$$\begin{aligned} &Circ \subset V1(r_1; [p_l^0, p_l^1]_{l=1}^n) + V2(r_2; [p_l^2, p_l^3]_{l=1}^n) \\ &\subset V(\max(r_1, r_2); [p_l^0, p_l^1, p_l^2, p_l^3]_{l=1}^n) \end{aligned} \tag{5}$$

The GJK algorithm is an efficient and reliable iterative algorithm for computing the Euclidean distance and the nearest points between a pair of convex polyhedral. The inner primitives of SSCH are convex hulls, it has the characteristics of convex hulls. The GJK algorithm easily is adopted to SSCH. As the distance between the SSCH $V(r^i, \{p_k^i\}_{k=1}^{n_i})$ and $V(r^j, \{p_k^j\}_{k=1}^{n_j})$ is given by the distance of the convex hull pair minus both extension radius.

$$\begin{aligned} &dis(V(r^i, \{p_k^i\}_{k=1}^{n_i}), V(r^j, \{p_k^j\}_{k=1}^{n_j})) = \\ &GJK(conv\{p_k^i\}_{k=1}^{n_i}, conv\{p_k^j\}_{k=1}^{n_j}) - r^i - r^j \end{aligned} \tag{6}$$

Fig.2 describes the SSCH of braking movement and the potential contact points between the manipulator and an obstacle.

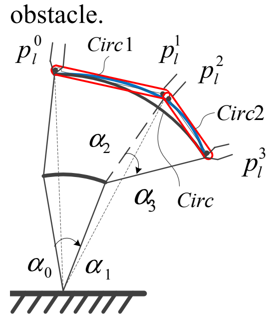

Fig.1 Approximate process of the braking trajectory

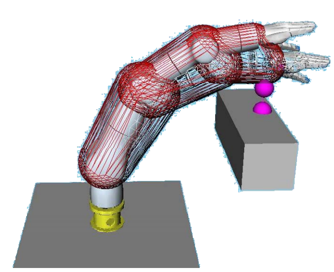

Fig. 2 Security distance and potential contact points between a manipulator and an obstacle

III. Collision Risk Assessment based on Fuzzy Theory

The collision risk degree of manipulators is related to the contact force of collision points, which is determined by various factors such as the nearest distance, the braking performance, the contact state, the movement state and control mode of robot, and so on. Establishing an accurate contact force model is very complicated, and it is also difficult to give an accurate result in the limited control period of robot. In this section, we introduce the fuzzy mathematical methodology to build a collision risk degree model, and design a more effective safety assessment system.

Five basic elements are selected to build a factor indicator set $U = \{D, T, \rho\}$, which includes three factor indicators such as the security distance D, the time of reaching collision

Authorized licensed use limited to: University of Florida. Downloaded on January 14,2021 at 17:31:59 UTC from IEEE Xplore. Restrictions apply.

points T and the radius of curvature of contact surface ρ. The factor indicator set can accurately reflect the collision risk degree of robots. Moreover, the indicators are irrelevant to each other.

*1) Security Nearest Distance **D***: The indicator reflects the possibility of collision in spaces. It is depended on three elements including the nearest distance, the braking performance and the control mode of manipulators. In this paper, we mainly consider two kinds of control mode, impedance control and position control. The impedance control can improves the security of the manipulator by controlling its stiffness/compliance. Because there is no obvious linear relationship between the control mode and the collision risk, it is integrated into the indicator ***D***.

*2) Time of Reaching Collision Points **T***: The indicator is introduced to deal with the influence of motion state on the collision risk. It is equal to the security nearest distance divided by the relative velocity along its direction, and reflects the urgency of occurring the collision.

3) Radius of Curvature ρ: The indicator mainly consider the influence of contact state on collision risk. It describes the sharpness of the contact surfaces.

A five-grade assessment vector set V={very danger, danger, normal, safety, very safety} is established to evaluate the collision risk of the current motion state. According to the experiences of operators, the evaluation standard of collision risk index based on D, T and ρ indicators are established (see Table I). We apply the fuzzy distribution method to construct the membership function of each indicators, which is directly related to the reliability and accuracy of the fuzzy synthetic evaluation.

TABLE I
EVALUATION STANDARD OF COLLISION RISK INDEX

Indicators	Very danger	Danger	Normal	Safety	Very safety
D (mm)	0	20~40	60~120	140~280	>300
T(s)	0	1~2	3~4	5~7	>8
ρ (mm)	<5	10~20	30~60	70~140	>150

It is obvious that the collision risk degree of manipulators is increased with the decrease of security nearest distance D. For the position control mode, when the security nearest distance D is less than 0, the collision risk is maximum. Fig.3(a) describes the corresponding membership function of the D indicator, it is defined by

$$r_{VD(D)} = \begin{cases} 1 & x \le 0 \\ \frac{1}{2} - \frac{1}{2}\sin\frac{\pi}{20}(x-10) & 0 < x < 20 \\ 0 & x \ge 20 \end{cases} \tag{7}$$

$$r_{D(D)} = \begin{cases} \frac{1}{2} + \frac{1}{2}\sin\frac{\pi}{20}(x-10) & 0 \le x < 20 \\ 1 & 20 \le x < 40 \\ \frac{1}{2} - \frac{1}{2}\sin\frac{\pi}{20}(x-50) & 40 \le x < 60 \end{cases} \tag{8}$$

$$r_{N(D)} = \begin{cases} \frac{1}{2} + \frac{1}{2}\sin\frac{\pi}{20}(x-50) & 40 \le x < 60 \\ 1 & 60 \le x \le 120 \\ \frac{1}{2} - \frac{1}{2}\sin\frac{\pi}{20}(x-130) & 120 < x \le 140 \end{cases} \tag{9}$$

$$r_{S(D)} = \begin{cases} \frac{1}{2} + \frac{1}{2}\sin\frac{\pi}{20}(x-130) & 120 \le x < 140 \\ 1 & 140 \le x \le 280 \\ \frac{1}{2} - \frac{1}{2}\sin\frac{\pi}{20}(x-290) & 280 < x \le 300 \end{cases} \tag{10}$$

$$r_{S(D)} = \begin{cases} 0 & x < 280 \\ \frac{1}{2} + \frac{1}{2}\sin\frac{\pi}{20}(x-290) & 280 \le x \le 300 \\ 1 & x > 300 \end{cases} \tag{11}$$

For the impedance control mode, we can control the stiffness/compliance of the manipulator, it allow to generate a certain position error. The error is roughly equal to f / k_t, where f is the allowable contact force and k_t is the stiffness coefficient. Thus compare with the position control mode, the membership function of the D indicator under the impedance control mode moves f / k_t mm to the left, as shown in Fig.3(b).

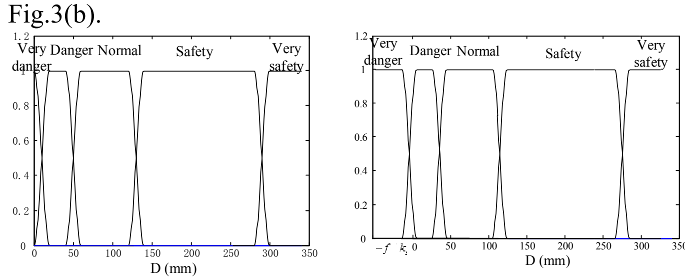

(a) Position control (b) Impedance control

Fig.3 Membership function of the ***D*** indicator under different control modes

According to Table I defines the membership function of the T indicator, as shown in Fig.4. For the ρ indicator, the trapezoidal fuzzy distribution is applied to establish a membership function (see Fig.5). Then a fuzzy evaluation matrix R of the three indicators is constructed, the matrix reflects the fuzzy correlation relationship from the evaluation indicator set U to the assessment vector set V.

$$R = \begin{bmatrix} r_{(D)} \\ r_{(T)} \\ r_{(K)} \end{bmatrix} = \begin{bmatrix} r_{VD(D)} & r_{D(D)} & r_{N(D)} & r_{S(D)} & r_{VS(D)} \\ r_{VD(T)} & r_{D(T)} & r_{N(T)} & r_{S(T)} & r_{VS(T)} \\ r_{VD(K)} & r_{D(K)} & r_{N(K)} & r_{S(K)} & r_{VS(K)} \end{bmatrix} \tag{12}$$

Authorized licensed use limited to: University of Florida. Downloaded on January 14,2021 at 17:31:59 UTC from IEEE Xplore. Restrictions apply.

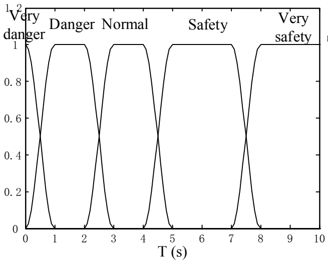

Fig.4 Membership function of the ***T*** indicator

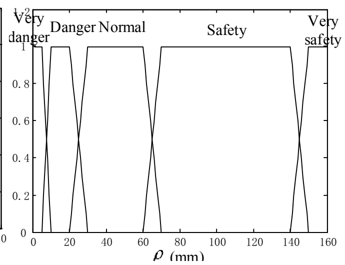

Fig. 5 Membership function of the ρ indicator

In the evaluation process, different factor indicators have different contributions to the collision risk, therefore these factor indicators can be given different weights by a weight set $A=\left[a_D \quad a_T \quad a_K\right]$ and $0<a_D<1$, $0<a_T<1$, $0<a_K<1$, $a_D+a_T+a_K=1$. According to the expert evaluation method, the weight set is determined $A=\left[0.4 \quad 0.4 \quad 0.2\right]$. we then chose the operator $M\left(\bullet,\oplus\right): b_j=\min(1,\sum_{i=1}^{n}(a_i \bullet r_{ij}))$, which is the weighted and summing operator to obtain the fuzzy synthetic evaluation results.

$$B=A\circ R=[a_D \quad a_T \quad a_K]\circ\begin{bmatrix} r_{VD(D)} & r_{D(D)} & r_{N(D)} & r_{S(D)} & r_{VS(D)} \\ r_{VD(T)} & r_{D(T)} & r_{N(T)} & r_{S(T)} & r_{VS(T)} \\ r_{VD(K)} & r_{D(K)} & r_{N(K)} & r_{S(K)} & r_{VS(K)} \end{bmatrix}$$
$$=\left\{b_{VD},b_D,b_N,b_S,b_{VS}\right\} \tag{13}$$

This operator may weaken the function of the main factors, but it can make full use of the information. Assuming the score of different grade in the assessment vector set V is $C=\{c_1,c_2,\cdots c_n\}$, Finally, the total score for every evaluation indicator can be calculated as

$$V=\sum_{i=1}^{n}c_i b_i \bigg/ \sum_{i=1}^{n}c_i \tag{14}$$

According to the total score, we can make a judgment for the collision risk degree of manipulators.

IV. EXPERIMENT

A System overview

To verify the validity of the proposed collision detection method based on fuzzy synthetic evaluate, the experiments have been performed on HIT's humanoid robot with 49 DOFs, as shown in Fig. 13. The humanoid robot is composed of a mobile base, a 2-DOF wrist, a 3-DOF head, two 15-DOF HIT-DLR dexterous hands and two 7-DOF anthropomorphic manipulators for dexterous work. It uses the control structure of upper computer and lower computer. The lower computer is to completed the control of all joints and the acquisition of sensor data in the 2ms control cycle. The humanoid robot's arms and hands may adopt the position control and impedance control mode. The upper computer is a computer with an Intel Core 2 Duo Processor E7500 (2.93GHz) and 8G DDR2. The proposed method is implemented on the upper computer, its control cycle is 100ms. The upper computer and the lower computer use wireless LAN communication.

B Position control mode

The six braking manoeuvres that occurred are listed in Table II. It shows the predictive braking distance and actual braking distance of single joint at different motion conditions, and demonstrates that the braking distance compute is conservative and precise.

TABLE II
PREDICTIVE AND ACTUAL BRAKING DISTANCE OF DIFFERENT MOTION CONDITIONS

No.	Velocity ($^\circ/s$)	Acceleration ($^\circ/s^2$)	Actual braking distance ($^\circ$)	Predictive braking distance ($^\circ$)
1	8	0	0.180	0.187
2	10	0	0.225	0.242
3	12	0	0.286	0.300
4	15	0	0.363	0.3937
5	10	2	0.229	0.2424
6	10	4	0.2308	0.2431

The desired trajectories of the right arm are shown in Fig.6. The novel method is used to evaluate the self-collision risk degree between the right arm and body of the humanoid robot. In the position control mode, building the collision detection model base on SSCH, the security nearest distance D between the arm and body of the humanoid robot and the T indicator can be obtained, as shown in Fig.7 and Fig.8. The radius of curvature ρ of the possible contact surface is 32mm. Assuming that the assessment set of the collision risk degree is $C=\{-2,-1,0,1,2\}$, the obtained collision risk degree is shown in Fig.9. Experimental results show that even if the shortest distance between the components is very close, the collision risk degree between the manipulator and body is decreased with the decrease of the manipulator velocity. Finally the total score of the collision risk is 0.4, the humanoid robot is relatively safe.

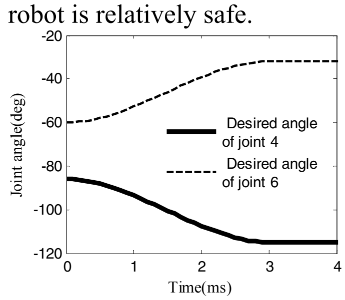

Fig.6 Desired trajectories of the right arm

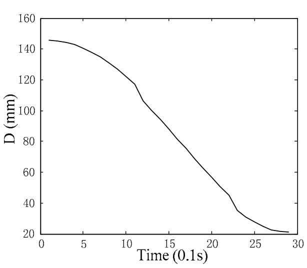

Fig.7 Change of the security nearest distance ***D*** indicator

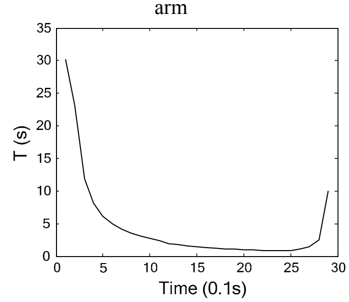

Fig.8 The change of the ***T*** indicator

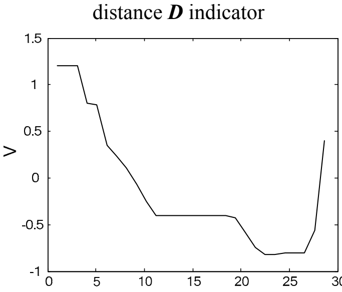

Fig.9 Safety assessment results in the experimental process

C Impedance control mode

Authorized licensed use limited to: University of Florida. Downloaded on January 14,2021 at 17:31:59 UTC from IEEE Xplore. Restrictions apply.

To verify the validity of the proposed method in the impedance control mode. On the basic of the previous experiment, the desired angle of joint 6 is changed to -37°, so that the right arm and the body can generate contact. The manipulator adopts the Cartesian impedance control. The desired contact force is 10N, the stiffness is 1000N/m, thus the allowed position error is 10mm. Fig.10 describes the change of the security nearest distance D in the experiment. The target positions of the manipulator are inside the humanoid robot, the heavy line in Fig.11 shows the collision risk degree in the position control mode, its value exceeds -1, so the humanoid robot is in danger of collision. Fig.12 shows the experimental process and the possible contact points. The dotted line in Fig.13 is the collision risk index in the impedance control mode. The collision risk degree is increased with the decrease of the distance between the manipulator and body in the motion process, the evaluated total score reaches a minimum before the collision occurs, but doesn't exceed -1, which means that the collision risk degree of the robot doesn't exceed the danger grade, the experimental results show that the obtained collision risk degrees of the robot by using the proposed method are consistent with the actual situation of the robot. After the contact occurs, it is difficult to obtain the change of speed and position of robot, so the information of tactile sensors is used to evaluate the collision risk degree of robots. Fig.13 shows the evaluated result under the impedance control mode and the actual robot state.

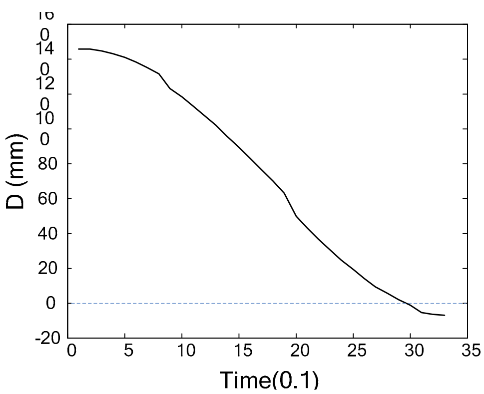

Fig.10 The change of the security nearest distance ***D*** indicator in impedance control mode

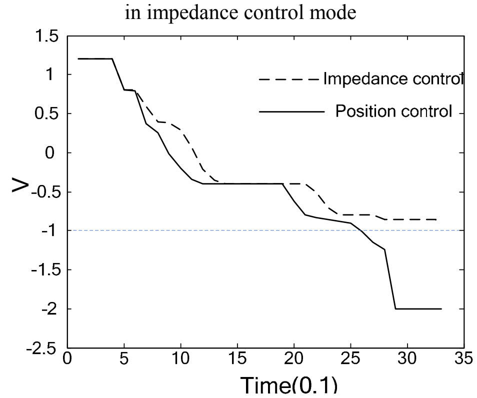

Fig.11 Comparison of collision risk index in the impedance control mode and the position control mode

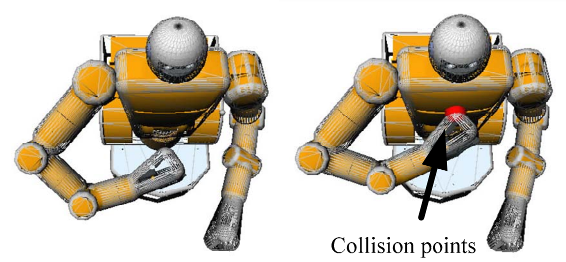

Fig.12 The experimental process and the possible contact points in the position control mode

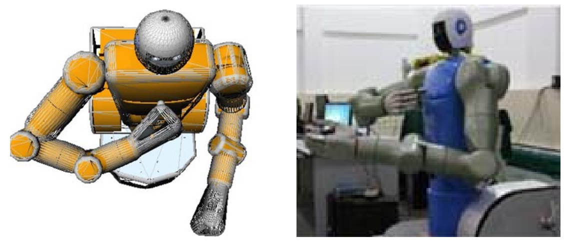

Fig.13 the safety assessment result under the impedance control mode and the actual robot state

V. CONCLUSION

In this paper, a new mathematical model for judging the collision risk degree of manipulators is established by using the fuzzy synthetic evaluate method, which contains three factor indicators D, T and ρ, comprehensively considers the effect of five factors on robot collision risk. Finally, a more objectively and accurately collision risk index is obtained. Future work will concentrate on developing a safety trajectory planner of robots using the safety assessment results.

ACKNOWLEDGMENT

This work was partially supported by Natural Science Foundation of China (Grant.51305097 and Grant.51505469) and supported by Overall innovation project of Shaanxi province science and technology plan resources leading technology industry (chain) project (Grant 2013KTCL01-02).

REFERENCES

[1] K. Okada, M. Inaba, M. Inoue, "Real-time and precise self-collision detection system for humanoid robots," *Proceedings of 2005 International Conference on Robotics and Automation*, 2005, pp. 1072-1077.

[2] K. Okada, M. Inaba, "A hybrid approach to practical self collision detection system of humanoid robot," *Proceedings of 2006 IEEE/RSJ International Conference on Intelligent Robots and Systems*, 2006, pp. 3952-3957.

[3] S. Gottschalk, M. C. Lin, D. Manocha, "Obbtree: A hierarchical structure for rapid interference detection," *Proceedings of International Conference on Computer Graphics and Interactive Techniques*, 1996, 23, pp. 171-180.

[4] K. Steinbach, J. Kuffner, T. Asfour, et al, "Efficient Collision and Self-Collision Detection for Humanoids Based on Sphere Tree Hierarchies," *Proceedings of 2006 IEEE-RAS International Conference on Humanoid Robots*, 2006, pp 560-566.

[5] L. Balan, G. M. Bone, "Real-Time 3D Collision Avoidance Method for Safe Humanand Robot Coexistence." *Proceedings of the 2006 IEEE/RSJ*

Authorized licensed use limited to: University of Florida. Downloaded on January 14,2021 at 17:31:59 UTC from IEEE Xplore. Restrictions apply.

International Conference on Intelligent Robots and Systems, 2006, pp, 276-282.

[6] M. Y. Ju, J. S. Liu, S. P. Shiang, et al, “Fast and Accurate Collision Detection Based on Enclosed Ellipsoid,” *Robotica*, 2001, vol. 19, no. 4, pp. 381-394.

[7] J. A. Corrales, F. A. Candelas, F. Torres, “Safe Human-Robot Interaction Based on Dynamic Sphere-Swept Line Bounding Volumes,” *Robotics and Computer-Integrated Manufacturing*, 2011, vol. 27, no.1, pp. 177-185.

[8] M. Schwienbacher, T. Buschmann, S. Lohmeier, et al, “Self-collision Avoidance and Angular Momentum Compensation for a Biped Humanoid Robot,” *Proceedings of 2011 IEEE International Conference on Robotics and Automation,* 2011, pp. 581–586.

[9] A. Hildebrandt, R. Wittmann, D. Wahrmann, et al, “Real-Time 3D Collision Avoidance for Biped Robots,” *Proceedings of 2013 IEEE/RSJ International Conference on Intelligent Robots and Systems*. 2013, pp: 4184-4190.

[10]H. Sugiura, M. Gienger, H. Janssen, et al, “Real-Time Collision Avoidance with Whole Body Motion Control for Humanoid Robots,” *Proceedings of the 2007 IEEE/RSJ International Conference on Intelligent Robots and Systems*, 2007, pp. 2053-2058

[11]O. Stasse, A. Escande, N. Mansard, S. Miossec, et al, “Real-Time (Self)-Collision Avoidance Task on a HRP-2 Humanoid Robot,” *2008 IEEE International Conference on Robotics and Automation*, 2008, pp. 3200-3205

[12]J. J. Kuffner, K. Nishiwaki, Kagami S, et al. “Self-Collision Detection and Prevention for Humanoid Robots,” *Proceedings of 2002 IEEE International Conference on Robotics and Automation*, 2002, pp. 2265-2270.

[13]B. Mirtich, “V-Clip: Fast and Obust Polyhedral Collision Detection,” *ACM Transactions on Graphics*, 1998, vol. 17, no. 3, pp. 177-208.

[14]S. Cameron, “Enhancing GJK: Computing Minimum and Penetration Distances between Convex Polyhedral,” *Proceedings of 1997 International Conference on Robotics and Automation*, 1997, pp. 3112-3117.

[15]H. Täubig, B. Bäuml, U. Frese. “Real-time Swept Volume and Distance Computation for Self-collision Detection,” *Proceedings of the 2011 IEEE/RSJ International Conference on Intelligent Robots and Systems*, 2011, pp. 1585-1592.

[16]H. Täubig, B. Bäuml B, U. Frese. “Real-time Continuous Collision Detection for Mobile Manipulators–A General Approach,” *Proceedings of the 12th IEEE-RAS International Conference on Humanoid Robots,* 2012, pp. 461-468.

Authorized licensed use limited to: University of Florida. Downloaded on January 14,2021 at 17:31:59 UTC from IEEE Xplore. Restrictions apply.